Electronic Supplementary Material (ESI) for Journal of Materials Chemistry A.

Supporting Information

A Facile and Broadly Applicable $CdBr_2$-Passivating Strategy for Halide Migration-Inhibiting Perovskite Films and High-Performance Solar Cells

Xiangnan Sun[a], Xitao Li[a], Haotong Li[a], Yao Li[a], Siqi Li[a], Yan-Zhen Zheng*[a] and Xia Tao*[a]

[a] State Key Laboratory of Organic-Inorganic Composites, Beijing University of Chemical Technology, 15 Beisanhuan East Road, Beijing 100029, P.R. China

* Corresponding author. Tel: +86-10-6445-3680 Fax: +86-10-6443-4784

E-mail: taoxia@mail.buct.edu.cn, taoxia@yahoo.com; zhengyz@mail.buct.edu.cn

Experimental section

Characterizations

Thin Film Characterization: UV-vis absorption spectra of perovskite film on the glass were recorded using a Perkin Elmer Lambda 950 UV/VIS spectrophotometer over the 300-900 nm wavelength range. PL and TRPL were obtained on an Edinburgh Instruments FLS 980 with an excitation wavelength of 470 nm. The crystallinity of the perovskite films was characterized using powder X-ray diffractometer (Rigaku, D/max 2500 VB25/PC) with CuKα radiation (λ = 0.15406 nm) at a scan rate of $5°\cdot min^{-1}$. The perovskite film morphology was analyzed using scanning electron microscope (SEM, JEOL-7610F) and atom force microscopy (AFM, Bruker Metrology Nanoscope III-D). The energy-dispersive spectroscopy (EDS) was measured using an X-ray energy dispersive spectrometer mounted on a JEOL-7610F microscope. The XPS and UPS measurements were carried out by Kratos X-ray photoelectron spectrometer (ThermoFisher ESCALAB 250Xi) equipped with monochromatic Al Kα (1,486.6 eV) and non-monochromatic HeI (21.22 eV) sources.

Device Characterization: The current density-voltage (*J-V*) characteristics were measured using a solar simulator (Oriel Sol3A) with the Keithley 2400 source meter under AM1.5G. The *J-V* curves were measured in the ambient atmosphere with a scan rate of 50 mV s^{-1}. The external quantum efficiency (EQE) spectrum was measured using an EQE system (Oriel instruments) with 150 W xenon lamp (USHIO, Japan) as a source of monochromatic light. The electrochemical impedance spectroscopy (EIS) measurement and other electrochemical testing were measured by using an electrochemical workstation (Zennium 400147). The EIS measurements were recorded on a Zahner electrochemical work station set to a frequency ranging from 10^6 Hz to 10

Hz in the dark state. All SCLC tests were measured at room temperature under dark conditions.

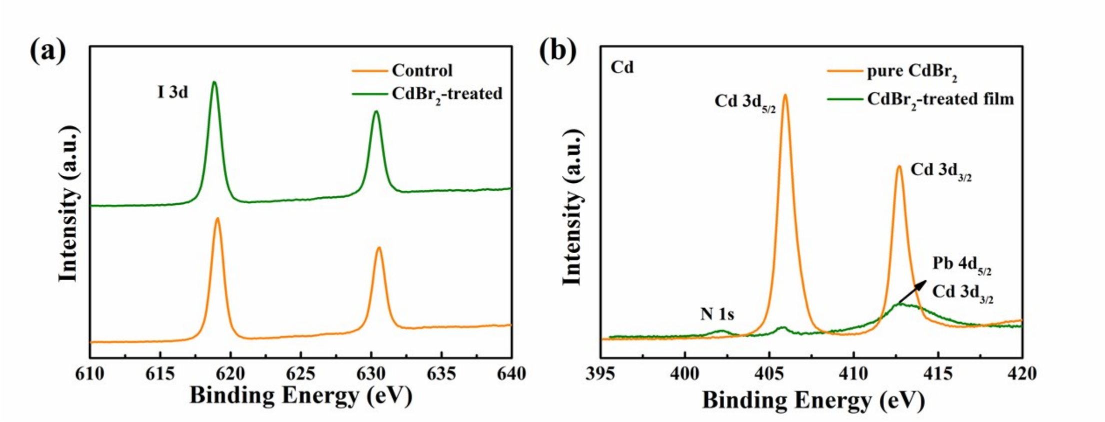

Fig. S1 (a) I 3d for perovskite films with and without the $CdBr_2$ treatment. (b) Cd 3d for $CdBr_2$-treated perovskite film and pure $CdBr_2$.

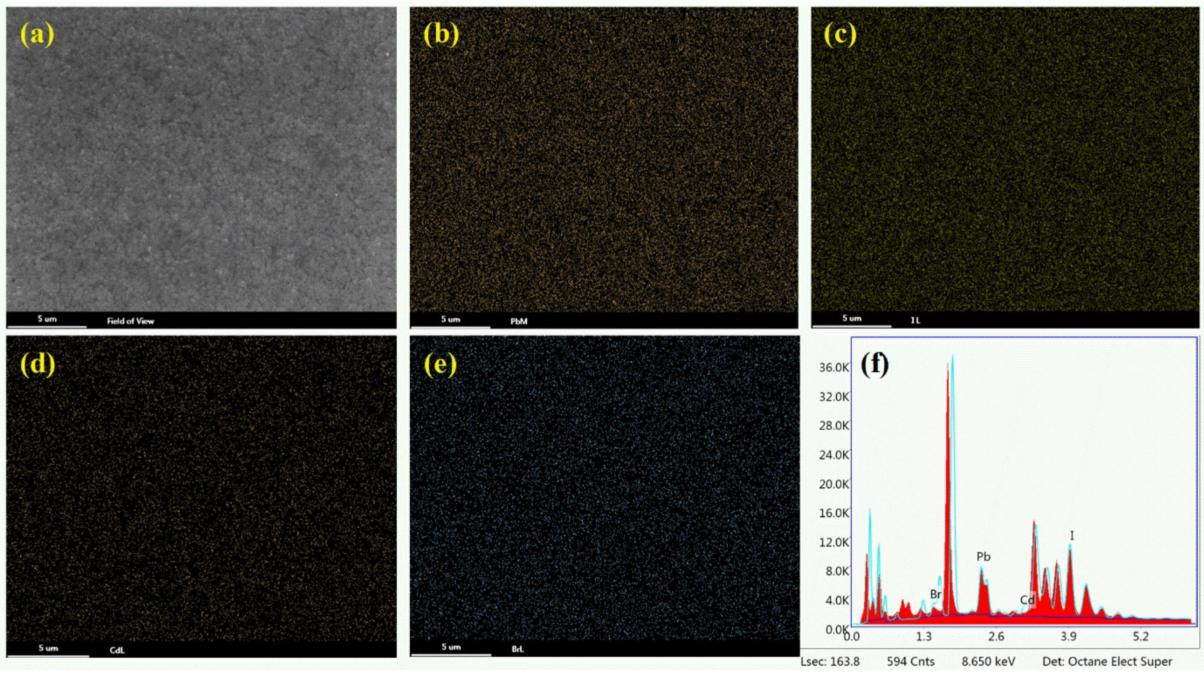

Fig. S2 SEM-EDS mappings of Pb, I, Cd and Br elements for the $CdBr_2$ modified perovskite film deposited onto the ITO substrate.

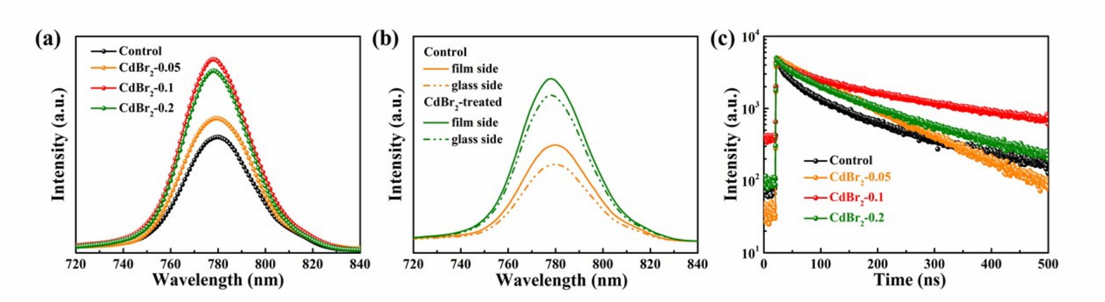

Fig. S3 (a) Steady state PL spectra of the perovskite films depending on $CdBr_2$ concentration. (b) Steady state PL spectra collected from the film and glass side of the perovskite film without and with $CdBr_2$-treated. (c) time-resolved PL decay spectra of the perovskite films depending on $CdBr_2$ concentration.

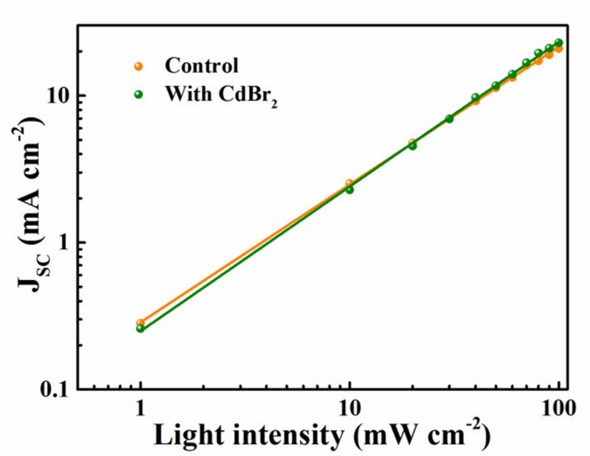

Fig. S4 J_{SC} versus light intensity for the PSCs with and without $CdBr_2$ treatment.

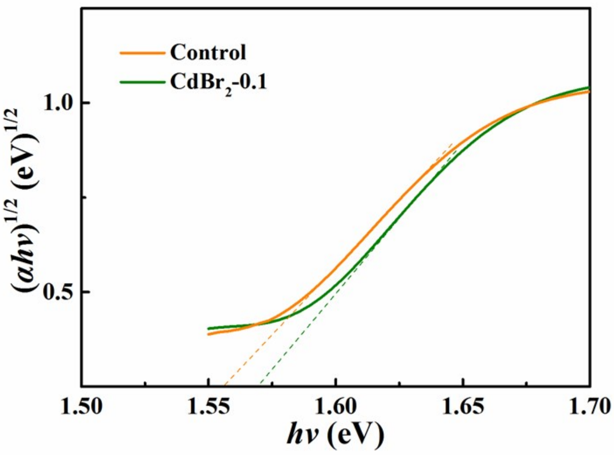

Fig. S5 $(\alpha h\nu)^{1/2}$ as a function of photo energy of perovskite films with and without $CdBr_2$-treated.

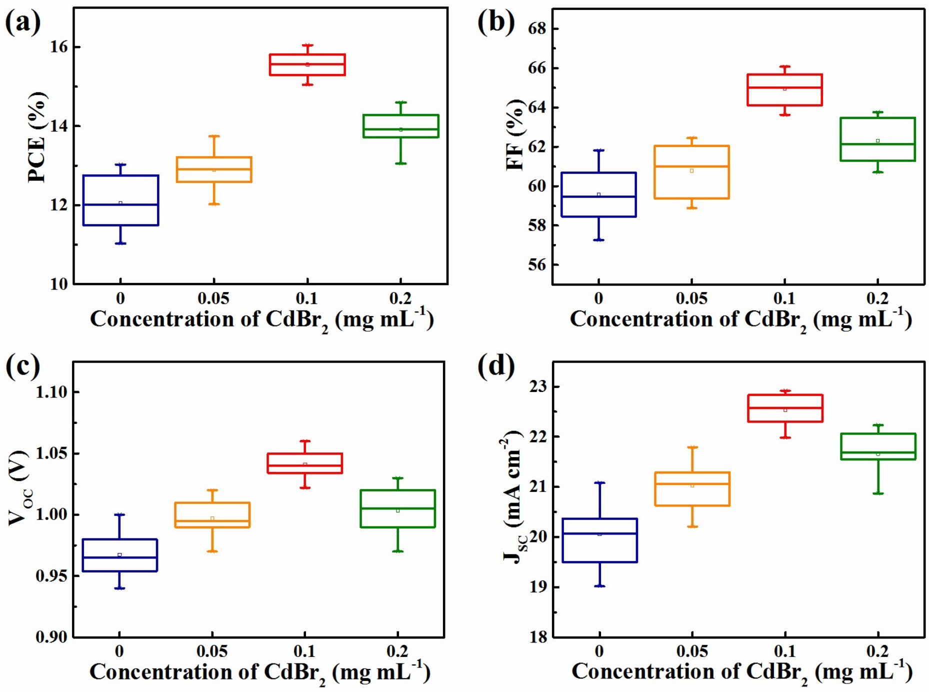

Fig. S6 Photovoltaic parameters statistics distribution of (a) PCE, (b) FF, (c) V_{OC}, (d) J_{SC} for the devices prepared from the four different perovskite films. (40 devices were collected from the different batch).

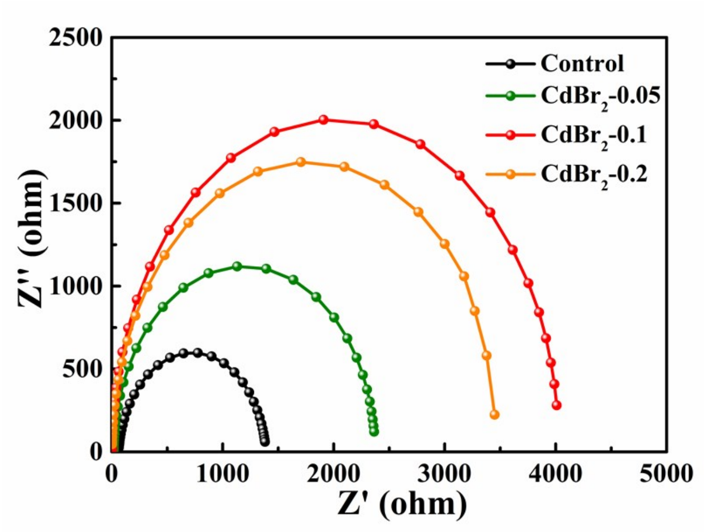

Fig. S7 Nyquist plots at bias 0.80 V of the perovskite devices with different concentration $CdBr_2$-treated under dark conditions.

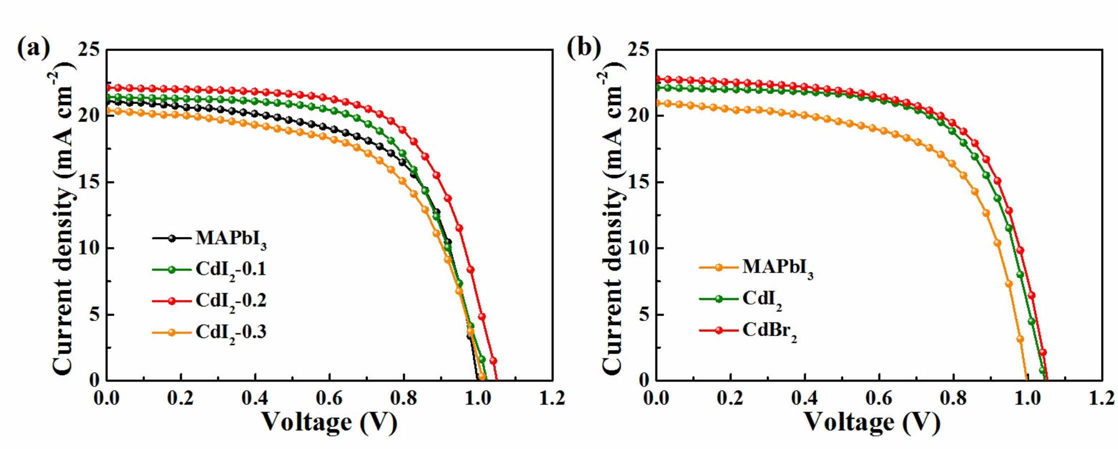

Fig. S8 (a) *J-V* curves of PSCs with different concentration CdI_2-treated. (b) *J-V* curves of the champion PSCs with $CdBr_2$ and CdI_2 treatment.

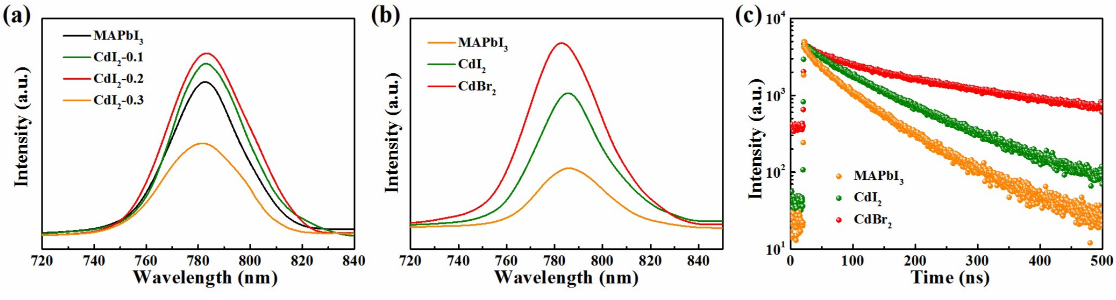

Fig. S9 (a) PL spectra of the perovskite films depending on CdI_2 concentration. (b) PL spectra of the control, CdI_2 and $CdBr_2$-treated perovskite films. (c) TRPL spectra of the perovskite films depending on $CdBr_2$ concentration.

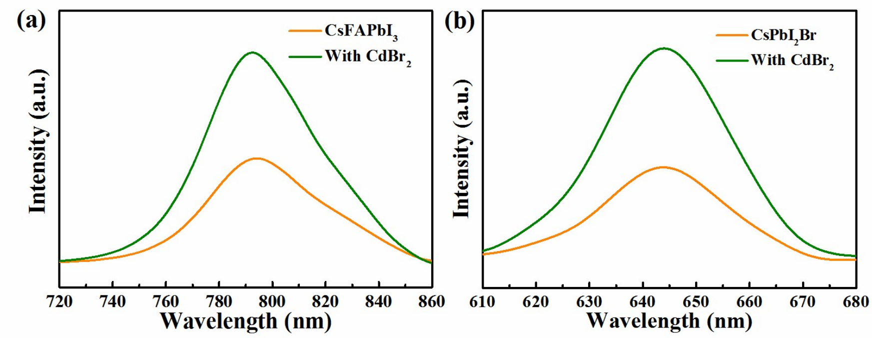

Fig. S10 PL spectra of the control and $CdBr_2$-treated (a) $CsFAPbI_3$ perovskite film and (b) $CsPbI_2Br$ perovskite film.

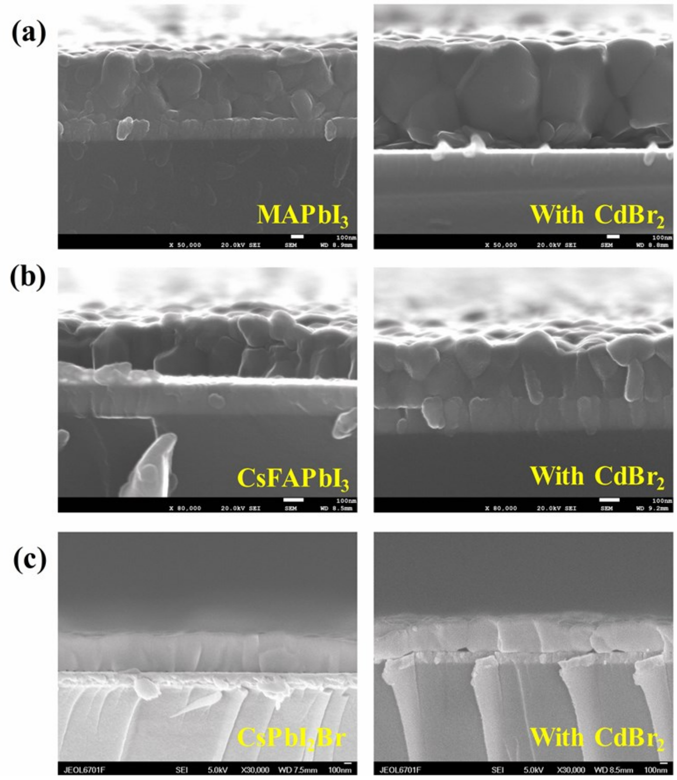

Fig. S11 The cross-sectional SEM images of (a) $MAPbI_3$ films, (b) $CsFAPbI_3$ films and (c) $CsPbI_2Br$ films without or with $CdBr_2$-treated.

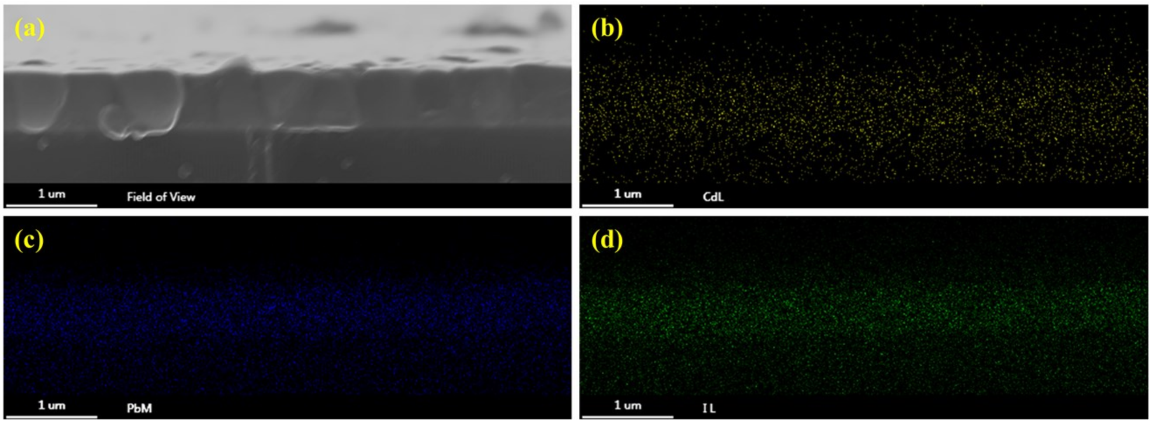

Fig. S12 Cross-sectional SEM-EDS mappings of Cd, Pb and I elements for the $CdBr_2$-treated perovskite film.

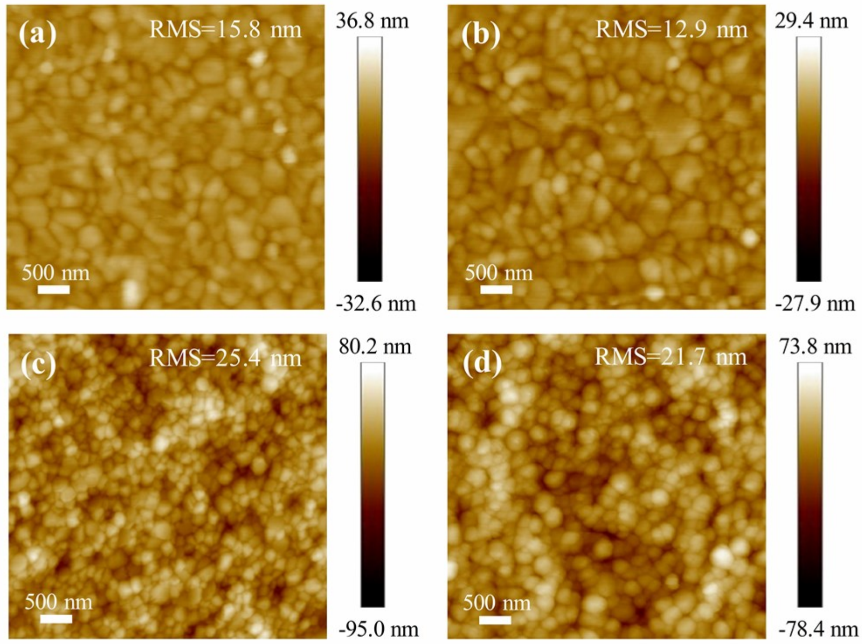

Fig. S13 AFM images of (a and b) $MAPbI_3$ perovskite films without and with $CdBr_2$-treated, (c and d) $CsFAPbI_3$ perovskite films without and with $CdBr_2$-treated.

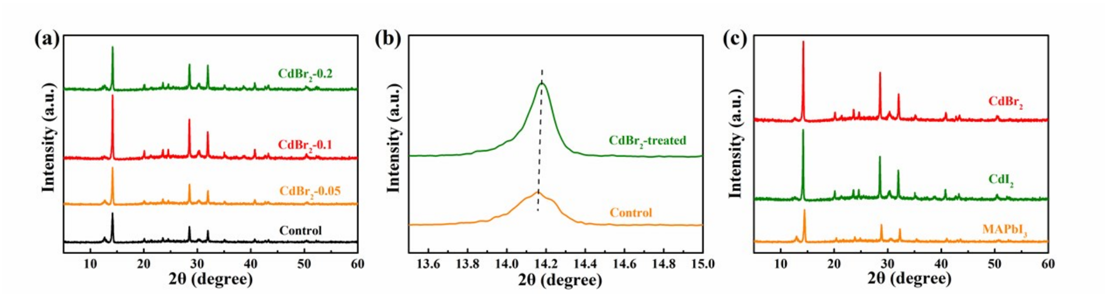

Fig. S14 (a) XRD patterns of the different concentration $CdBr_2$-treated perovskite films. (b) The (110) peak of $CdBr_2$-treated perovskite film. (c) XRD patterns of the control and $CdBr_2$- or CdI_2-treated perovskite films.

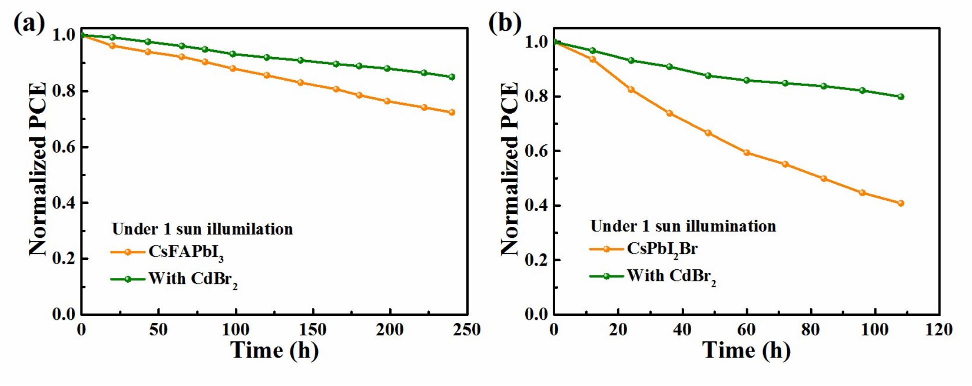

Fig. S15 Long-term stability measurements of (a) $CsFAPbI_3$-based devices and (b) $CsPbI_2Br$-based devices without encapsulation under one sun illumination at room temperature in N_2.

Table S1 The specific percentage of X/Pb atomic ratio.

Samples	Name	Atomic%
Control	Pb	15.33
	I	39.24
Treated	Pb	15.58
	I+Br	43.78

Table S2 Parameters of the TRPL spectroscopy based on the perovskite films with different concentrations of $CdBr_2$-treated.

Samples	τ_1	% of τ_1	τ_2	% of τ_2	τ_{ave}
Control	28.26	14.34	135.90	85.66	120.46
$CdBr_2$-0.05	43.90	6.65	118.09	93.35	113.16
$CdBr_2$-0.1	36.11	6.61	221.47	93.39	209.22
$CdBr_2$-0.2	35.58	10.19	151.49	89.81	139.68

Table S3 Photovoltaic parameters of C-PSCs with or without $CdBr_2$ treatment measured in both reverse and forward scan.

PSCs		V_{oc} (V)	J_{sc} (mA cm^{-2})	FF (%)	η (%)	HI
Control	RS	1.00	21.08	61.82	13.03	14.2%
	FS	0.96	20.06	58.14	11.19	
$CdBr_2$-0.1	RS	1.06	22.92	66.08	16.05	5.2%
	FS	1.05	22.30	64.95	15.21	

*The hysteresis index (HI) was calculated to quantify the hysteresis level according to the following equation:

$$HI = \frac{PCE_{RS} - PCE_{FS}}{PCE_{RS}}$$

Table S4 Photovoltaic parameters of PSCs with different concentration CdI_2 treatment.

PSCs	V_{oc} (V)	J_{sc} (mA cm^{-2})	FF (%)	η (%)
Control	1.00	20.94	61.70	12.91
CdI_2-0.1	1.02	21.41	63.20	13.86
CdI_2-0.2	1.04	22.24	64.35	14.88
CdI_2-0.3	1.01	20.39	59.72	12.54

Table S5 Parameters of the TRPL spectroscopy based on the different perovskite films without or with $CdBr_2$-treated.

Samples	τ_1	% of τ_1	τ_2	% of τ_2	τ_{ave}
$CsFAPbI_3$	14.27	33.61	33.38	66.39	26.96
$CsFAPbI_3$-$CdBr_2$	21.79	37.77	44.11	62.23	35.68
$CsPbI_2Br$	5.60	12.39	43.84	87.61	39.10
$CsPbI_2Br$-$CdBr_2$	1.29	0.47	61.09	99.53	60.80

Table S6 Summary of key related information about the PSCs (structure similar to this work)

Perovskite component	PSC structure	PCE (%)	Date	Ref
$MAPbI_3$	ITO/SnO_2/PVK/Co_3O_4@NC/C	14.63%	2021.02	1
$Cs_{0.05}(FA_{0.85}MA_{0.15})_{0.95}Pb(I_{0.85}Br_{0.15})_3$	FTO/SnO_2/PVK/MWCNT(1 cm^2)	11.2%	2021.02	2
$MAPbI_3$	FTO/c-TiO_2/m-TiO_2/PVK/C	11.91%	2020.06	3
$MAPbI_3$	FTO/TiO_2/PVK/C	14.10%	2020.07	4
$MAPbI_2Cl$	FTO/c-TiO_2/m-TiO_2/PVK/C	11.70%	2019.01	5
$CsFA_{0.83}MA_{0.17}PbI_{2.53}Br_{0.47}$	FTO/SnO_2/PVK/CuSCN/C	15.3%	2020.03	6
$MAPbI_3$	FTO/c-TiO_2/m-TiO_2/PVK/C	15.21%	2019.03	7
$FA_{0.8}Cs_{0.2}PbI_{2.64}Br_{0.36}$	FTO/c-TiO_2/m-TiO_2/PVK/PEO/C	14.9%	2019.04	8
$FA_{0.85}MA_{0.15}PbI_{2.85}Br_{0.15}$	FTO/c-TiO_2/m-TiO_2/PVK/C	14.41%	2019.01	9
$MAPbI_3$	ITO/HMB-C_{60}/PVK/C	16.03%	2019.06	10
$MAPbI_3$	FTO/c-TiO_2/m-TiO_2/PVK/NiO/C	13.6%	2019.05	11

$Cs_{0.05}FA_{0.81}MA_{0.14}PbI_{2.55}Br_{0.45}$	$ITO/SnO_2(QDs)/PVK/C$	13.64%	2020.03	12
$MAPbI_3$	$FTO/TiO_2/PVK$-SWCNT/SWCNT-C	15.73%	2019.01	13
$Cs_X(MA_{0.7}FA_{0.3})_{1-X}PbI_3$	$FTO/c\text{-}TiO_2/m\text{-}TiO_2/PVK/C$	15.03%	2019.01	14
$Cs_{0.05}FA_{0.81}MA_{0.14}PbI_{2.55}Br_{0.45}$	$FTO/c\text{-}TiO_2/m\text{-}TiO_2/PVK/C$	15.09%	2020.06	15
$MAPbI_3$	$FTO/ZnO\text{-}RGO\text{-}CuInS_2/PVK/Au$	15.74%	2020.06	16
$MAPbI_3$	$ITO/SnO_2/PVK/CdBr_2/C$	16.05%		This work

Notes and references

1 C. Geng, P. Wei, H. Chen, H. Liu, S. Zheng, H. Wang and Y. Xie, *Chem. Eng. J.*, 2021, **414**, 128878.

2 R. Chen, Y. Feng, L. Jing, M. Wang, H. Ma, J. Bian and Y. Shi, *J. Mater. Chem. C*, 2021, **9**, 3546-3554.

3 T. Xu, K. Zou, X. Sun, Z. Wan, H. Tang, Y. Zhang, L. Chen, Q. Qiao and W. Huang, *Mater. Lett.*, 2020, **275**, 128157.

4 Q.-Q. Chu, Z. Sun, B. Ding, K. Moon, G.-J. Yang and C.-P. Wong, *Nano Energy*, 2020, **77**, 105110.

5 S. Sajid, A. M. Elseman, D. Wei, J. Ji, S. Dou, H. Huang, P. Cui and M. Li, *Nano Energy*, 2019, **55**, 470-476.

6 Y. Yang, M. T. Hoang, D. Yao, N. D. Pham, V. T. Tiong, X. Wang, W. Sun and H. Wang, *Sol. Energy Mater. Sol. Cells*, 2020, **210**, 110517.

7 Y. Xiao, C. Wang, K. K. Kondamareddy, P. Liu, F. Qi, H. Zhang, S. Guo and X.-Z. Zhao, *J. Power Sources*, 2019, **422**, 138-144.

8 Z. Wu, Z. Liu, Z. Hu, Z. Hawash, L. Qiu, Y. Jiang, L. K. Ono and Y. Qi, *Adv. Mater.*, 2019, **31**, 1804284.

9 C. Wu, K. Wang, Y. Jiang, D. Yang, Y. Hou, T. Ye, C. S. Han, B. Chi, L. Zhao, S. Wang, W. Deng and S. Priya, *Adv. Funct. Mater.*, 2021, **31**, 2006803.

10 J. Zhou, J. Hou, X. Tao, X. Meng and S. Yang, *J. Mater. Chem. A*, 2019, **7**, 7710-7716.

11 C. Cai, K. Zhou, H. Guo, Y. Pei, Z. Hu, J. Zhang and Y. Zhu, *Electrochim. Acta*, 2019, **312**, 100-108.

12 S.N. Vijayaraghavan, J. Wall, L. Li, G. Xing, Q. Zhang and F. Yan, *Mater. Today Phys.*, 2020, **13**, 100204.

13 Y. Wang, H. Zhao, Y. Mei, H. Liu, S. Wang and X. Li, *ACS Appl. Mater. Interfaces*, 2019, **11**, 916-923.

14 P. Liu, Y. Gong, Y. Xiao, M. Su, S. Kong, F. Qi, H. Zhang, S. Wang, X. Sun, C. Wang and X.-Z. Zhao, *Chem. Commun.*, 2019, **55**, 218-221.

15 L. Gao, J. Hu, F. Meng, Y. Zhou, Y. Li, G. Wei and T. Ma, *J. Colloid Interf. Sci.*, 2020, **579**, 425-430.

16 R. Taheri-Ledari, K. Valadi and A. Maleki, *Prog. Photovolt. Res. Appl.*, 2020, **28**, 956-970.